



HAL
open science

A signature for turbulence driven magnetic islands

O. Agullo, M. Muraglia, A Poyé, S. Benkadda, M Yagi, X. Garbet, A. Sen

► **To cite this version:**

O. Agullo, M. Muraglia, A Poyé, S. Benkadda, M Yagi, et al.. A signature for turbulence driven magnetic islands. *Physics of Plasmas*, 2014, 10.1063/1.4894699 . hal-01793854

HAL Id: hal-01793854

<https://hal.science/hal-01793854v1>

Submitted on 17 May 2018

HAL is a multi-disciplinary open access archive for the deposit and dissemination of scientific research documents, whether they are published or not. The documents may come from teaching and research institutions in France or abroad, or from public or private research centers.

L'archive ouverte pluridisciplinaire **HAL**, est destinée au dépôt et à la diffusion de documents scientifiques de niveau recherche, publiés ou non, émanant des établissements d'enseignement et de recherche français ou étrangers, des laboratoires publics ou privés.

A signature for turbulence driven magnetic islands

O. Agullo, M. Muraglia, A. Poyé, S. Benkadda, M. Yagi, X. Garbet, and A. Sen

Citation: *Physics of Plasmas* (1994-present) **21**, 092303 (2014); doi: 10.1063/1.4894699

View online: <http://dx.doi.org/10.1063/1.4894699>

View Table of Contents: <http://scitation.aip.org/content/aip/journal/pop/21/9?ver=pdfcov>

Published by the AIP Publishing

Articles you may be interested in

[Simultaneous use of camera and probe diagnostics to unambiguously identify and study the dynamics of multiple underlying instabilities during the route to plasma turbulence](#)

Rev. Sci. Instrum. **85**, 11E813 (2014); 10.1063/1.4890250

[The effect of diamagnetic flows on turbulent driven ion toroidal rotation](#)

Phys. Plasmas **21**, 056106 (2014); 10.1063/1.4872322

[Gyrokinetic simulation of momentum transport with residual stress from diamagnetic level velocity shears](#)

Phys. Plasmas **18**, 042504 (2011); 10.1063/1.3579481

[Turbulence driven magnetic reconnection causing long-wavelength magnetic islands](#)

Phys. Plasmas **17**, 072308 (2010); 10.1063/1.3463435

[Resistive pressure gradient-driven turbulence at stellarator plasma edge](#)

Phys. Plasmas **4**, 3282 (1997); 10.1063/1.872469



2014 Special Topics

PEROVSKITES

2D MATERIALS

MESOPOROUS MATERIALS

BIOMATERIALS/
BIOELECTRONICS

METAL-ORGANIC
FRAMEWORK
MATERIALS

AIP | APL Materials

Submit Today!

A signature for turbulence driven magnetic islands

O. Agullo,^{1,2} M. Muraglia,^{1,2} A. Poyé,³ S. Benkadda,^{1,2} M. Yagi,⁴ X. Garbet,⁵ and A. Sen⁶

¹Aix-Marseille Université, CNRS, PIIM, UMR 7345 Marseille, France

²France-Japan Magnetic Fusion Laboratory, LIA 336 CNRS, Marseille, France

³Univ. Bordeaux, CNRS, CEA, CELIA (Centre Lasers Intenses et Applications), UMR 5107, F-33405 Talence, France

⁴Plasma Theory and Simulation Gr., JAEA, Rokkasho, Japan

⁵IRFM, CEA, St-Paul-Lez-Durance 13108, France

⁶Institute for Plasma Research, Bhat, Gandhinagar 382428, India

(Received 3 June 2014; accepted 25 August 2014; published online 8 September 2014)

We investigate the properties of magnetic islands arising from tearing instabilities that are driven by an interchange turbulence. We find that such islands possess a specific signature that permits an identification of their origin. We demonstrate that the persistence of a small scale turbulence maintains a mean pressure profile, whose characteristics makes it possible to discriminate between turbulence driven islands from those arising due to an unfavourable plasma current density gradient. We also find that the island poloidal turnover time, in the steady state, is independent of the levels of the interchange and tearing energy sources. Finally, we show that a mixing length approach is adequate to make theoretical predictions concerning island flattening in the island rotation frame. © 2014 AIP Publishing LLC. [<http://dx.doi.org/10.1063/1.4894699>]

I. INTRODUCTION

In fusion devices, confinement can be affected by various instabilities acting at different time and spatial scales. In particular, a magnetic tearing instability can lead to the generation of magnetic islands that can reach a macroscopic width whereas at smaller scales, interchange like instabilities usually generate turbulence.¹ An important issue is the understanding of the interaction between turbulence and islands. Indeed, for an efficient control of neoclassical tearing modes (possibly a stabilization) and therefore an avoidance of disruptions, one needs to develop a clear understanding of the multiscale mechanisms that are involved. In the past decades, island properties and turbulence characteristics have typically been studied independently except in a few theoretical papers^{2–6} where turbulence has been assumed to act on the islands through an enhancement of transport parameters. However, the problem needs to be addressed in a self consistent manner since the island and the turbulence influence each other's evolutions through a mutual interaction. As it has been shown in Refs. 7–10, a magnetic island can substantially modify the nature of turbulence and also possibly trigger new short wavelength micro-instabilities that can impact the transport properties of a plasma in the presence of a magnetic island. In particular, in this context, the existence and the calculation of turbulent viscosity have been investigated in Ref. 11. On the other hand, turbulence can affect the island dynamics and can even provide the necessary free energy to generate it through nonlinear mechanisms as has been discussed in Refs. 8 and 12–15. As of now there is no experimental proof that such a mechanism is indeed at work, although it could give some key explanations for the unexpected onset of islands. Indeed, while (3,2) NTM magnetic islands, in the core of the plasma, are often triggered by sawtooth precursors,¹⁶ (2, 1) magnetic islands can appear without any noticeable MHD event or any

current driven instability.¹⁷ It follows that the determination of a specific signature of islands generated by turbulence would be useful to gather experimental evidence of these mechanisms and to improve the means for controlling islands in fusion devices.

In this paper, we aim to tackle this question by considering the generation of islands by resistive interchange turbulence and to extract any key features that differentiate these turbulence driven islands from the conventional current gradient driven magnetic islands. A second objective of our study is to clarify the interplay between zonal flow, diamagnetic effects, magnetic island and small scale instabilities. Our paper is organised as follows. Section II presents the model equations which include curvature parameters and diamagnetic effects and also provides details of the numerical procedures used to solve the model equations. In Sec. III, we discuss the origin of the zonal flows and the flattening of the tearing driven magnetic islands in the context of the model. In Sec. IV, we focus on turbulence driven islands. We review briefly the mechanisms generating them and present their elementary characteristics, including pressure flattening. In Sec. V, we analyze the origin of their rotation. We also discuss the interplay between interchange and island scales. In Sec. VI, we study the origin of the pressure flattening in both the early and the asymptotic nonlinear phases. We identify a key feature (signature) of a turbulence driven magnetic island that is linked to the pressure profile properties. We also propose a mixing length model to predict the island flattening. In Sec. VII, we present a discussion of our results and make some concluding remarks.

II. MULTISCALE INSTABILITIES MODEL

Our simulations are carried out on a minimal two-dimensional plasma model based on the two-fluid Braginskii equations in the drift approximation^{18,19} with cold ions and

isothermal electrons. The model includes magnetic curvature and electron diamagnetic effects:⁸

$$\frac{\partial}{\partial t} \nabla_{\perp}^2 \phi + \{\phi, \nabla_{\perp}^2 \phi\} = \{\psi, \nabla_{\perp}^2 \psi\} - \kappa_1 \frac{\partial p}{\partial y} + \mu \nabla_{\perp}^4 \phi, \quad (1)$$

$$\frac{\partial}{\partial t} \psi = \{\psi, \phi - p\} - v_{*} \frac{\partial \psi}{\partial y} + \eta \nabla_{\perp}^2 (\psi - \psi_0), \quad (2)$$

$$\frac{\partial}{\partial t} p + \{\phi, p\} = -v_{*} \left((1 - \kappa_2) \frac{\partial \phi}{\partial y} + \kappa_2 \frac{\partial p}{\partial y} \right) + \hat{\rho}^2 \{\psi, \nabla_{\perp}^2 \psi\} + \chi_{\perp} \nabla_{\perp}^2 p, \quad (3)$$

where the dynamical field quantities are the electrostatic potential ϕ , the electron pressure p and the total magnetic flux ψ (with $\psi_0 = \psi_0(x)$ denoting its equilibrium profile). The vorticity and the current in the parallel direction are, respectively, $\omega = \nabla_{\perp}^2 \phi$ and $j = \nabla_{\perp}^2 \psi$. The equilibrium consists of a constant pressure gradient and a magnetic field given by the Harris current sheet model,^{20,21} namely, $\mathbf{B}_0(x) = \tanh\left(\frac{x}{a}\right) \hat{y}$, where a determines the width of the profile. Details of the model can be found in Ref. 8. The numerical resolution of our simulations is up to 1024 grid points in the x (radial) direction and to 256 poloidal modes. In this study, we have fixed $\hat{\rho} = 0.058$, $v_{*} = 10^{-2}$, $\kappa_1 = 5$, $\kappa_2 = 0.36$ and the dissipative parameters (μ , χ_{\perp} , η) are all set equal to 10^{-4} .

We next categorize the most unstable interchange mode number by m_{*} and its growth rate by $\gamma_{m_{*}}$. In this work, the modes $m \geq 2$ are stable with respect to tearing instability and the parameter set imposes $m_{*} \gg 1$ when $\Delta' < 1.16$. The nature of the $m = 1$ mode, i.e., the radial parity, depends on the competition between the interchange and tearing instabilities. The stiffness of the magnetic equilibrium profile at the resonance (a^{-1} for the Harris magnetic equilibrium) modifies the growth rate of both interchange and tearing modes as well as the stability index parameter $\Delta'_{m=1} \equiv \Delta'$.²² If we take a as a control parameter and keep the box sizes constant, Δ' can be seen as a measure of the stiffness: the smaller the Δ' , the larger are m_{*} and $\gamma_{m_{*}}$ and the smaller the tearing instability growth rate γ_1^{\perp} .

We carry out a range of linear and nonlinear simulations with different values of Δ' . The linear growth rates $\gamma_1(\Delta')$ of the modes $m = 1$ and $m = m_{*}$ are given in Fig. 1. Note that

the tearing mode $m = 1$ is marginally stable or unstable but is weaker than interchange mode for $\Delta' \leq 1.16$. Linear spectra are shown in Fig. 2. For $\Delta' = -0.45$, the large scale $m = 1$ tearing instability is stable ($\gamma_1^{\perp} < 0$), $m_{*} = 17$, and a wide range of interchange unstable modes are present. In the case of $\Delta' = 1.16$, the dominant $m = 1$ linear mode is driven by a tearing instability and mode numbers $m \in$ (Refs. 2 and 13) are unstable with respect to the interchange instability.

III. TEARING DRIVEN ISLANDS

Before studying the impact of interchange instability on magnetic islands, we have to clarify the island properties in the absence of turbulence. Indeed, first, we need to highlight the differences with the extensively studied case where pressure fluctuations and curvature terms are neglected (see Ref. 23 and references there in). Second, we also want to verify to what extent the classical flattening mechanism of island, based on anisotropic diffusion considerations, is valid.²⁴ Let us focus on a situation where the $m = 1$ tearing instability is strongly dominant by considering the $\Delta' = 4.02$ case.

A. Generation of zonal flows

It has been shown²² that curvature leads nonlinearly to the generation of zonal flows (mean poloidal flows or ZF), with energy transfer occurring from the unstable tearing mode $m = 1$ through the Maxwell stress. A snapshot of the ZF is shown in Fig. 3. Note that it is slightly asymmetric in terms of parities. It concentrates also the energy of the flow, as indicated by the spectra shown for the same time. In fact, the origin of the zonal flows comes from curvature terms because they introduce a parity symmetry breaking²⁵ in the tearing mode structure. More precisely, in the minimal model for tearing instability $p = \kappa_i = v_{*} = 0$, zonal flows are not generated because the tearing mode satisfies, both in the nonlinear and linear regimes, the following well known symmetries: there exists y_{*} such that, for any δy , $\psi(x, y_{*} + \delta y, t) = \psi(x, y_{*} - \delta y, t)$ and $\phi(x, y_{*} + \delta y, t) = -\phi(x, y_{*} - \delta y, t)$. In the model (1–3), there is no such symmetry. Indeed, first, the fluid Larmor radius term and Maxwell stress generate, respectively, pressure fluctuations and vorticity perturbations localized at the resonant surface. The resulting

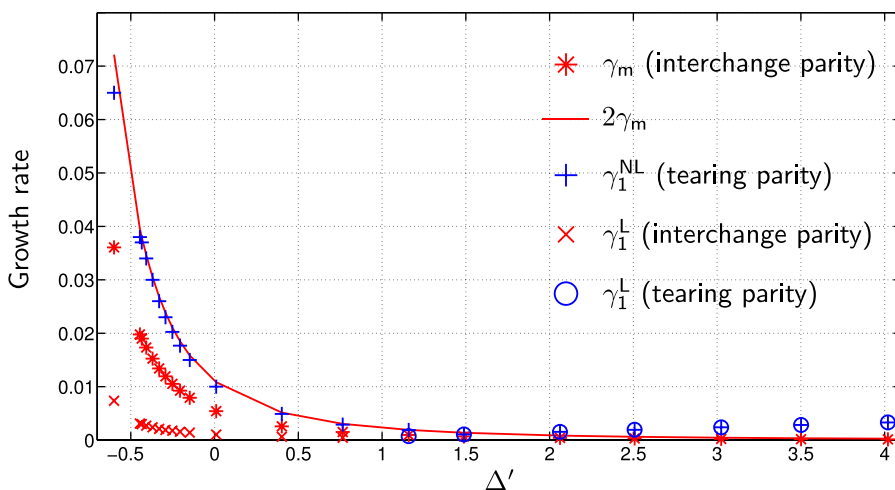


FIG. 1. Growth rates of the modes $m = 1$ and m_{*} obtained by linear and nonlinear simulations. The colors indicate the parity of the mode.

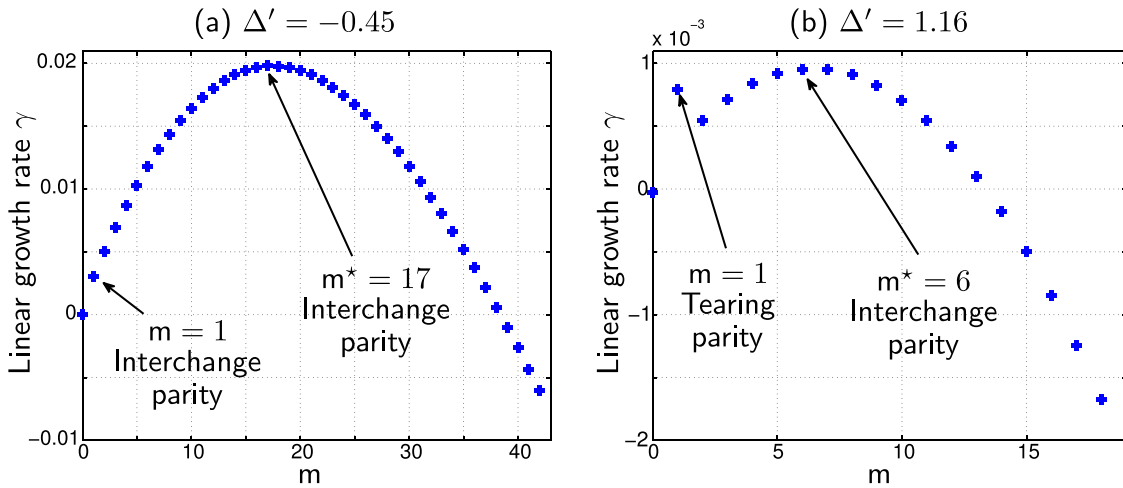


FIG. 2. Linear spectra: (a) $\Delta' = -0.45$, (b) $\Delta' = 1.16$.

potential, which depends also on the boundary conditions, is not localized. Second, pressure fluctuations are also amplified by the diamagnetic and curvature terms, which are proportional to ϕ but not to ω , and p . Therefore they also contain a non-localized part with radial extension, roughly, the size of the potential flow structure. The resulting two scale pressure structure does not present any global symmetry, even in the linear phase, as observed in the zoomed snapshot of the pressure in Fig. 3. Consequently, the $m=1$ tearing mode generates nonlinearly both zonal flow and mean pressure fluctuations. The latter contribute jointly to the flattening of the island observed in the last graph of Fig. 3.

B. Perturbed temperature profile and implicit thermal conductivity

The model contains implicitly a parallel conductivity¹⁹ and one might expect that it explains the pressure flattening when the island width becomes much larger than the critical island width $w_c = \sqrt{8}(\chi_{\perp}/\chi_{\parallel})^{1/4} \sqrt{a/k_y} \in [0.17, 0.34]$ for negative Δ' runs.²⁴ The implicit parallel diffusivity is defined as $\chi_{\parallel} \equiv \eta^{-1} \rho^2$ and Δ_{\parallel} is the operator $[\tilde{\psi}, [\tilde{\psi}, \cdot]]$. This parallel conductivity is in fact equal to the collisional parallel conductivity v_{Te}^2/ν_{ei} where v_{Te} is the thermal electron temperature and ν_{ei} the ion-electron collision frequency. Note that the model does not contain explicit collisional parallel conductivity. However, the ExB shear flow possibly contributes

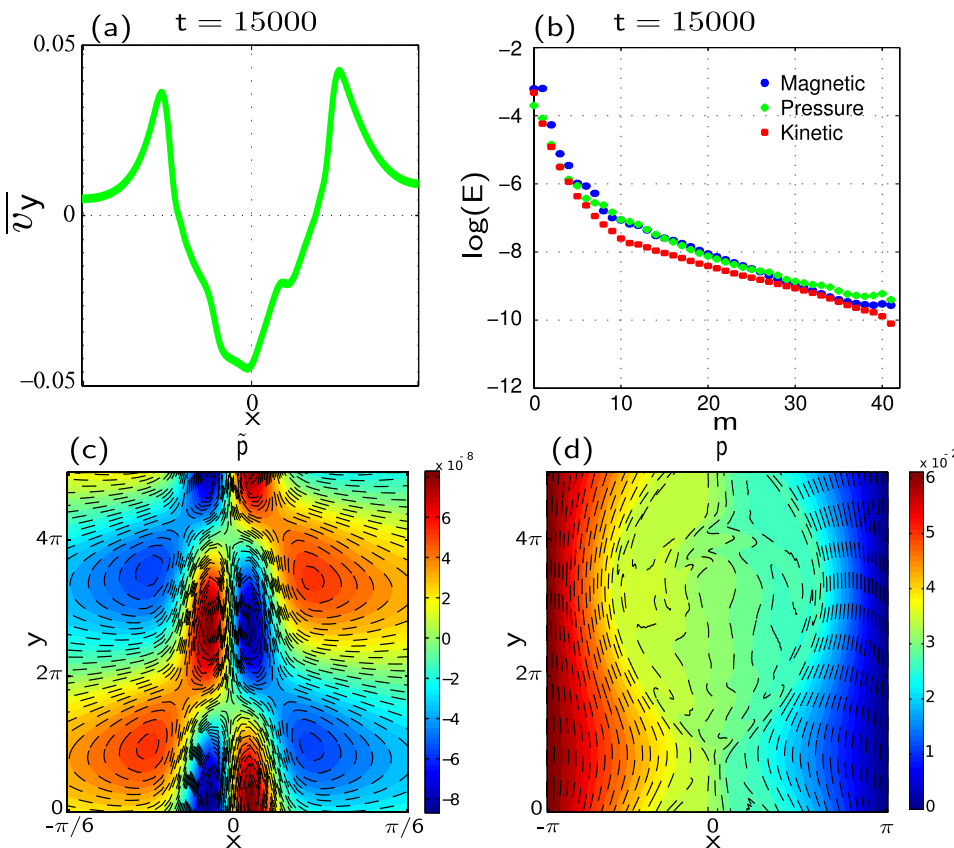


FIG. 3. $\Delta' = 4.02$. (a) Mean poloidal flow at $t = 15000$. (b) Spectra in the nonlinear phase at $t = 15000$. (c) Snapshot of the pressure fluctuations (zoom), in the linear phase at $t = 3000$. (d) Snapshot of the pressure at $t = 100000$.

to the flattening and not only to the island rotation. For instance, only the zonal flow part of the convective term $[\phi, p]$, $\phi'_{m=0} \partial_y p$, possibly accounts for the drive of pressure fluctuations at the island velocity. The flow is neglected in the Fitzpatrick model. To clarify the role of the flow and the implicit conductivity, let us consider the dominant terms in the pressure evolution equation. We find that when the tearing instability drives the dynamics, i.e., when Δ' is large enough, the fluid Larmor radius term dominates the pressure equation: in the nonlinear regime the following typical amplitudes for the different terms of the pressure equation are found $\partial_t p \sim \rho_*^2 [\psi, j - j_0] \sim 3.10^{-3} \gg [\phi, p] \sim 3.10^{-4} \geq$ other contributions ($\Delta' = 4.02$). To measure the link between the ExB flow and the island flattening, we carry out the study in the island rotating frame of reference. Let us therefore introduce the quantities $\tilde{p}(x, y_{\text{isl}}, t) = p(x, y, t)$ where $y_{\text{isl}} = y - v_{\text{isl}} t$ and $\tilde{\phi}_{\text{isl}} = \phi - v_{\text{isl}} x$. Here $v_{\text{isl}}(t)$ is the poloidal island velocity which is essentially the sum of the diamagnetic and the $E \times B$ velocities, including nonlinear fluctuations.²² In the island frame of reference and in the nonlinear regime, using the Ohm's law, we obtain

$$\partial_t \tilde{p} \sim \chi_{\parallel} \Delta_{\parallel} (\tilde{p} - \tilde{\phi}_{\text{isl}}) + \chi_{\parallel} [\tilde{\psi}, \partial_t \tilde{\psi}]. \quad (4)$$

Note that in terms of amplitudes, $\Delta_{\parallel} \tilde{\phi}_{\text{isl}} / \Delta_{\parallel} \phi \sim 10^{-2}$ in the nonlinear regime. However, by evaluating physical quantities in the island rotating frame, we eliminate the part of the electrostatic potential ϕ which drives the island rotation through $E \times B$ plasma velocity and focus on the possible role of the latter in the pressure flattening of the island. In Fig. 4 are shown snapshots of the parallel Laplacian of, both, the pressure and electrostatic fluctuations. First, one clearly observes that in the range of intermediate spatial scale structures, we tend to obtain a quasi-static equilibrium $\Delta_{\parallel} (\tilde{p} - \tilde{\phi}_{\text{isl}}) \sim 0$ asymptotically, which means that diffusion of pressure fluctuations along the field lines is compensated by electrostatic fluctuations. Let us emphasize however that the bracket $\chi_{\parallel} [\tilde{\psi}, \partial_t \tilde{\psi}]$ cannot be neglected even in the long

range dynamics and, notably, at such intermediate scales. Indeed, while magnetic fluctuations are poloidally pulled by both diamagnetic velocity and $E \times B$ flow, pressure fluctuations tend to be pulled by the $E \times B$ flow only. Structural stability of the island, i.e., the fact that pressure and magnetic fluctuations at island scales have to move at the same velocity, imposes therefore the permanent generation of fluctuations in the vicinity of the separatrices and also inside the island. The latter have a tendency to be aligned along the magnetic field because of the large parallel collisional conductivity, as observed also in Fig. 4, notably at the separatrices. As a consequence $\chi_{\parallel} [\tilde{\psi}, \partial_t \tilde{\psi}]$ remains one of the dominant terms. The Fitzpatrick model²⁴ does not take into account the impact of these fluctuations, what we term as structural fluctuations, on the island flattening. Second, and this is the important point, only relatively strong field aligned pressure fluctuations contribute to the Larmor nonlinear term $\hat{\rho}^2 [\psi, j]$ and therefore to the flattening of the pressure (see Fig. 4). Noting further that at the separatrices, the perpendicular diffusion, which is numerically at least a factor of three larger than the convective and linear terms, cannot be neglected, we see that the island structure is governed by

$$\chi_{\parallel} \Delta_{\parallel} \tilde{p} + \chi_{\perp} \Delta_{\perp} \tilde{p} \sim 0. \quad (5)$$

In this equation, we have neglected the impact of the structural fluctuations. Indeed, we can expect that statistically, they only act as a modulator of the island rotation. Moreover, an indirect way to show that they do not invalidate Fitzpatrick model and Eq. (5) is to consider overtone harmonics. Indeed, an enhancement of the first harmonics by coupling of/with the structural fluctuations could be produced. Fitzpatrick predictions²⁴ that the first overtone harmonics ($m > 1$) of the unstable mode are localized in the vicinity and inside the island, die away rapidly outside and have radial extensions roughly equal to the island size could become invalid. Validity is clearly verified in Fig. 5 where the harmonic $m = 1, 2, 3, 4$ are drawn. The ratio of the

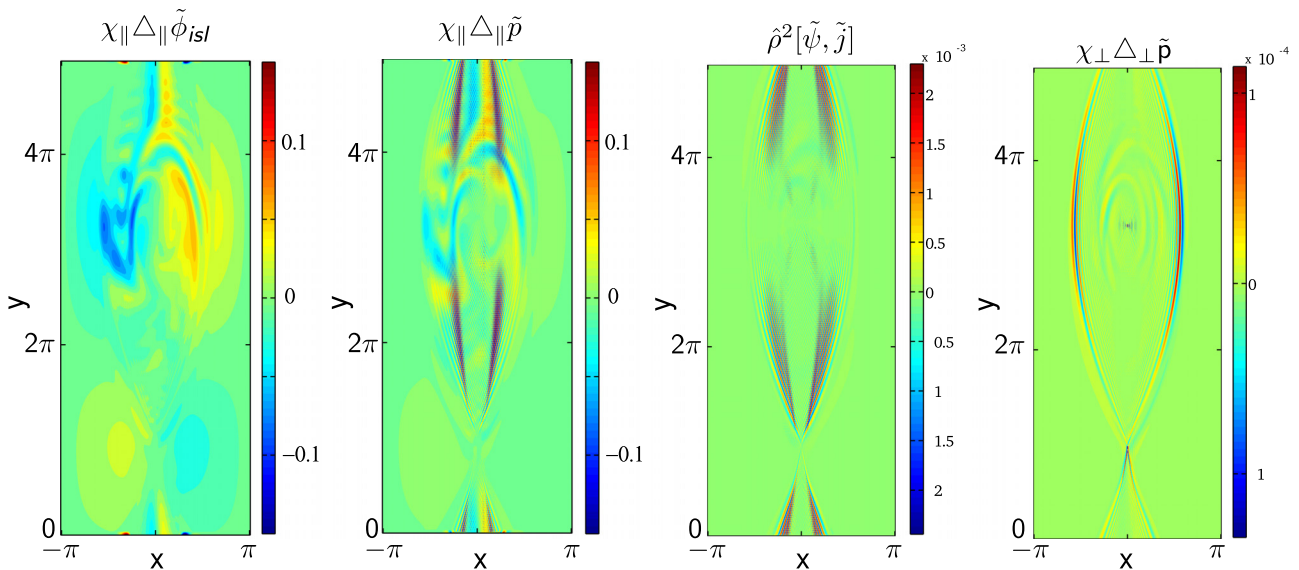


FIG. 4. $\Delta' = 4.02$, $t = 10^5 \tau_A$. Dominant parallel and perpendicular contributions in the pressure equation.

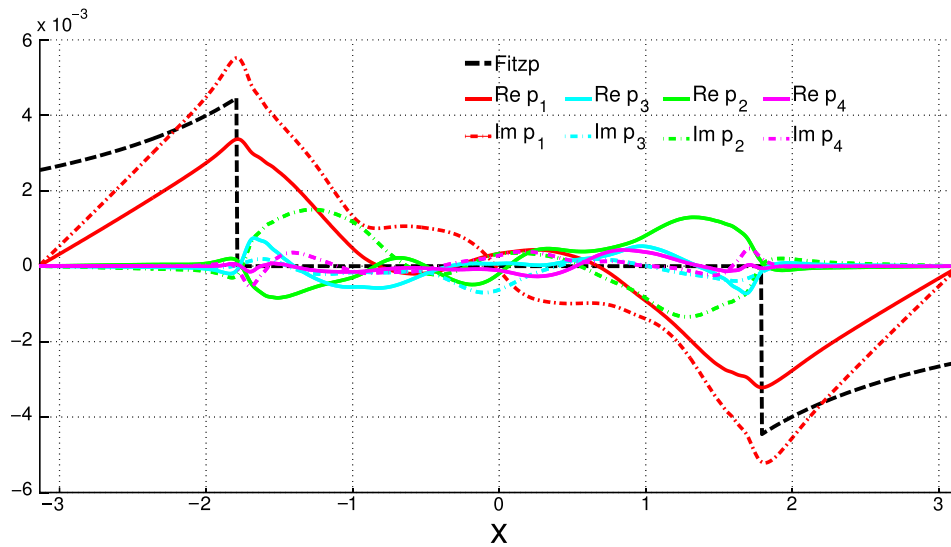


FIG. 5. Eigenfunctions of the pressure fluctuations for $\Delta' = 4.02$ and $t = 40000\tau_A$.

amplitude between $p_{m>1}$ and p_1 are also compatible with the predictions. The theoretical external $m = 1$ pressure eigenfunction²⁴ for the limit $w \ll x \ll L_x$ is also indicated (narrow dotted black line). It shows that the amplitude of the mode $m = 1$ has the expected order of magnitude at the edge of the island.

IV. TURBULENCE DRIVEN MAGNETIC ISLANDS

A. Nonlinear magnetic island generation

As explained in Ref. 8 and reviewed briefly here, a fast quasilinear formation of a magnetic island occurs at large scales. It is induced by small scale interchange instabilities, in particular when $\Delta' < 0$ or has moderate positive values. Figs. 6(a) and 6(b) show the time evolution of the energy for

both, interchange and large scale $m \leq 1$ modes. The latter dominates energetically asymptotically, while the former grows exponentially at a faster rate as soon as they enter in the nonlinear phase, when Δ' is negative or weakly positive (approximately $\Delta' \leq 1.7$ in the set of runs of this paper). We will call this phase the quasi-linear phase (QLP). Nonlinear growth rates can be therefore computed during this phase and are reported in Fig. 1 in order to compare them with the linear values. The color of the points indicates the parity of the mode. First, let us emphasize that the growth rate of the interchange mode m_* is not affected by the nonlinearities in this phase. Second, the growth of the $m = 1$ mode is amplified by the nonlinearities. In fact, the parity of the modes switches from an interchange parity in the linear phase to a tearing parity in the QLP. As a consequence, a magnetic

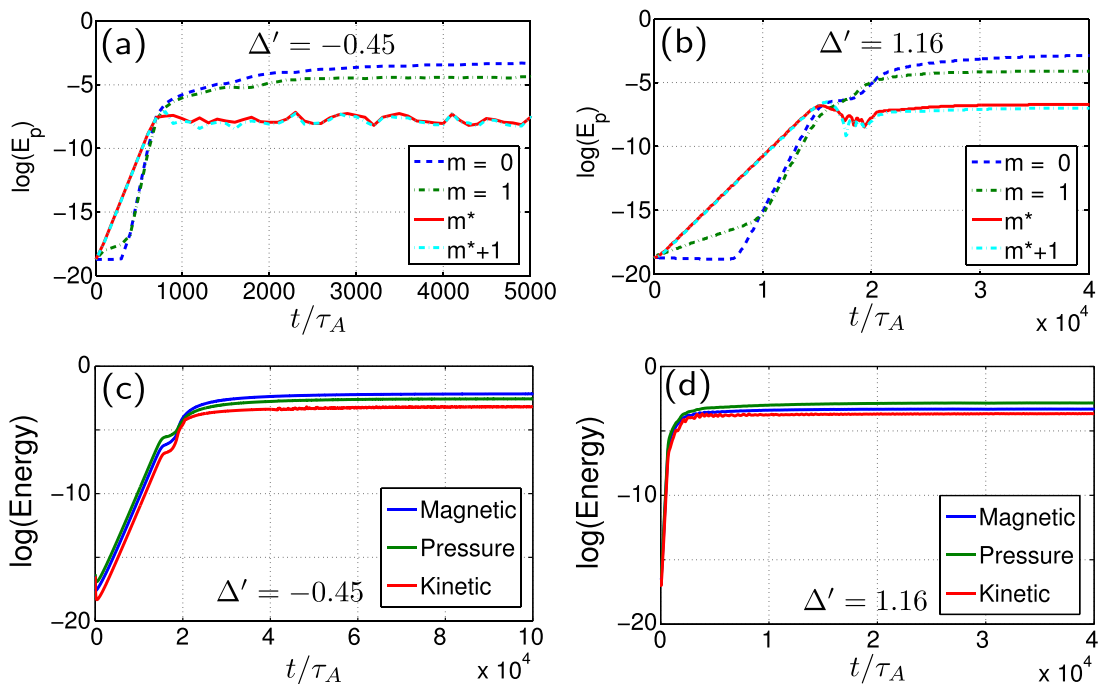


FIG. 6. (Left) $\Delta' = -0.45$. (Right) $\Delta' = 1.16$: Time evolution of the pressure fluctuations energy for modes $m \in \{0, 1, m_*, m_* + 1\}$ and total energies $E_m(t)$, $E_p(t)$ and $E_k(t)$.

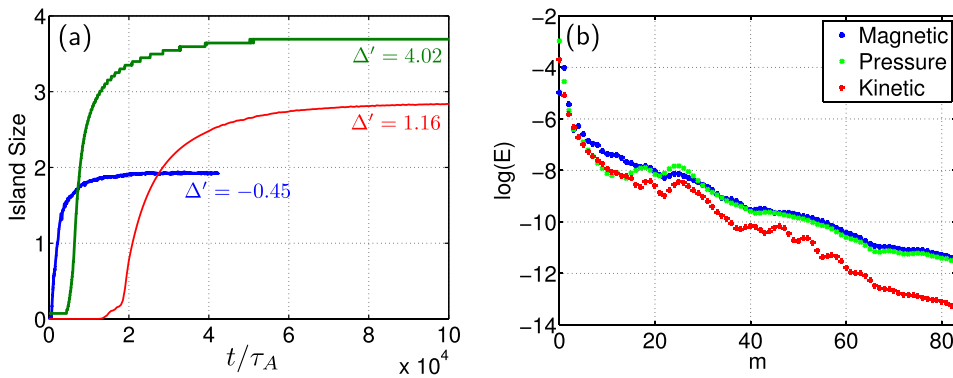


FIG. 7. (a) Island sizes versus time. (b) Spectra at $t=40000\tau_A$ and $\Delta' = -0.45$.

island is nonlinearly generated. Finally, Fig. 1 indicates that the nonlinear growth of the $m=1$ mode is determined by the small scale fluctuations according to $\gamma_1^{NL} \sim \gamma_{m_*} + \gamma_{m_* \pm 1} \sim 2\gamma_{m_*} > \gamma_1^L$. It shows that a nonlinear beating of the small scales interchange modes $m \sim m_*$ gives rise to the generation of a magnetic island at large scales. The resulting island size is however smaller than when the large scales are tearing unstable as can be seen in Fig. 7(a). This beating occurs because if initially, the system is driven by small-scale interchange modes I_{ss} , their mutual non linear interactions can only drive tearing parity large scale fluctuations T_{ls} . Indeed, all the quadratic terms in Eqs. (1)–(3) follows the following symmetry breaking: $\{I_{ss}, I_{ss}\} \rightarrow T_{ls}$.

Nonlinear properties of the magnetic island and, in particular, the characterization of the island size at saturation according to the level of turbulence have been investigated in Ref. 8 and will not be reported here. However, it is instructive to compare energetically, the cases $\Delta' < 0$ and $\Delta' > 0$. Figs. 6(c) and 6(d) show that pressure fluctuations dominate magnetic ones in intensity in the first case, while the converse occurs in the second case in the nonlinear phase. Let us emphasize, nevertheless, that when $\Delta' = 1.16$, the QLP is still driven by the small scale interchange instability, while in the nonlinear regime and on larger time scales, tearing instability drives predominantly the growth of the island.

B. Pressure flattening of magnetic islands by interchange mechanisms

Measured pressure fluctuations, similar to tearing driven islands, induce an island flattening, as observed in Fig. 8. From an experimental point of view, island formation is detected by measuring the temperature profiles at different poloidal positions using ECE or Thomson scattering methods.²⁶ However, according to Fig. 8, no clear difference between the two kinds of islands can be assessed in terms of pressure profiles at different poloidal positions. Nevertheless, the origin of the flattening, the underlying mechanisms, possibly differs in the two cases. We will investigate this question and look for some specific signatures of turbulence driven magnetic islands. Note that a first signature is that they grow at twice the interchange growth rate. In the tokamak context, such a growth is difficult to measure because it corresponds to a low level of magnetic fluctuations. Access to the q profile, at a given time, to

determine if there is a tearing instability or not is also difficult in experiments.²⁷

Thus, to proceed further and clarify the origin of pressure flattening, we need to discriminate between the nonlinear interactions driving it. However, we must take into consideration the fact that there is a pile up of kinetic energy at the largest scale $m \leq 1$ (see Fig. 7(b)). Similarly for tearing driven island cases, the generation of a persistent strong zonal flow, compared with other velocity fluctuations, requires us to make the analysis in the island frame. We therefore study, in the following, the poloidal island dynamics in the context of interchange turbulence.

V. POLOIDAL ISLAND ROTATION AND TURBULENCE

The rotation frequency of the tearing driven island is known to be modified by nonlinearities and has a strong dependence on the transport coefficients.²⁸ This can have a significant physical consequence, for example, in a tokamak, where such a nonlinear effect on the rotation can lead to a slowing down of the plasma through locking to the resistive wall producing in turn a degradation of the plasma and/or triggering a transport barrier.²⁹

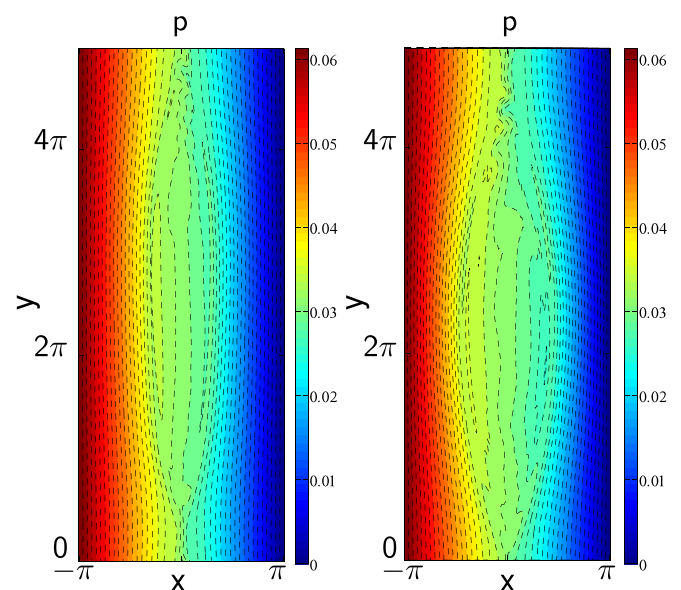


FIG. 8. Snapshots of the pressure in the stationary regimes: (Left) $\Delta' = -0.45$, $t = 4 \cdot 10^4 \tau_A$. (Right) $\Delta' = 1.16$, $t = 10^5 \tau_A$.

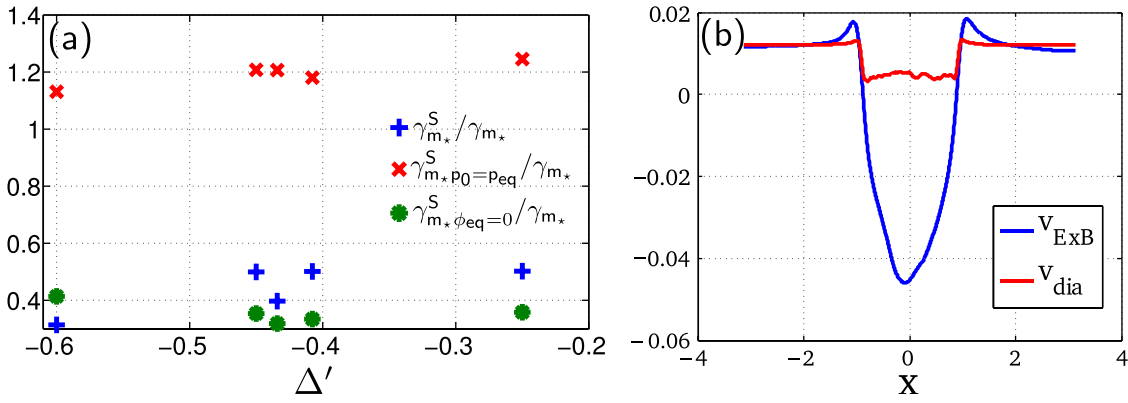


FIG. 9. (a) Normalised nonlinear instantaneous growth rate versus Δ' . (b) Diamagnetic and $E \times B$ velocity at $t = 42\,125\tau_A$ for $\Delta' = -0.45$.

However, the case of turbulent driven island has not been studied. Interchange mechanism should nonlinearly reduce the diamagnetic velocity $p'_0 \equiv p'_{m=0}(x)$ and generate a ZF. The latter should alter the level of the turbulence in the vicinity of the island by lowering the interchange energy source level in the nonlinear regime, whatever the nature of the island. Fig. 9 shows that in fact, contrary to the case of electrostatic turbulence and in the absence of islands, there is no $E \times B$ shear flow stabilisation.³⁰ turbulence is not mitigated by $E \times B$ shear flow but only by the lowering of the diamagnetic velocity. Indeed, first, it is found that the ratio $\gamma_{m_*}^s / \gamma_{m_*} < 1/2$ whatever be the value of Δ' . $\gamma_{m_*}^s$ is the growth rate computed by considering the mean profile, averaged in time, in the nonlinear asymptotic regime instead of the initial equilibrium. m_* remains essentially unchanged ($m_*^s \sim m_*$). Second, on the same graph, we observe that if we compute $\gamma_{m_*}^s$ neglecting the nonlinear diamagnetic effect, we find $\gamma_{m_*, p_0=p_{eq}}^s \sim \gamma_{m_*}$. The graphs $\gamma_{m_*, p_0=p_{eq}}^s / \gamma_{m_*}$ and $\gamma_{m_*, \phi_0=0}^s / \gamma_{m_*}$ as a function of Δ' show that the interchange growth rate is in fact weakly sensitive to the $E \times B$ mean flow. Indeed, the mean flow is a jet which is weakly sheared in the resistive layer surrounding the resonant surface where the unstable modes grow (see Fig. 9). Finally, we observe that pressure gradient stabilization of the small scales instability when Δ' is negative is such that the ratio $\gamma_{m_*}^s / \gamma_{m_*} \sim 0.4$ is almost constant, independent therefore of the level of the interchange energy source.

Let us now quantify how such modifications influence the poloidal island rotation when $\Delta' < 0$. Following Ref. 22,

to distinguish the terms driving the island rotation, we segregate the Ohm's law in its different contributions in terms of instantaneous frequency averaged on the current sheet and computed for the mode $m = 1$:

$$\omega_{tot} = \omega_* + \tilde{\omega}_* + \omega_{E \times B} + \omega_0 + \omega_\eta. \quad (6)$$

The RHS terms are, respectively, the linear and nonlinear part of the diamagnetic frequency, the $E \times B$ Doppler frequency, the contribution of the equilibrium magnetic field and the contribution of the resistivity. In this model, the direct contribution from modes $m > 1$ to island rotation is neglected. From this instantaneous frequency and/or the predicted island velocity $\omega_{tot} / k_{m=1}$, we can explicitly compute the island poloidal position as a function of time. In Fig. 10, the comparison between the model predictions and the measured position shows a good agreement, noting that the integration is done on a large time interval. In the nonlinear regime, there is almost one order of magnitude between $\omega_{E \times B}$ and the diamagnetic contribution: the $E \times B$ velocity drives the island in the ion diamagnetic direction. This is, of course, linked not only to the flattening of the pressure inside the island, which reduces the diamagnetic velocity, but also to the plasma jet generated by the turbulence in which the magnetic island structure is strongly frozen. Let us emphasize that the direction of the rotation is the result of various effects. In the case of tearing unstable magnetic island, it was found that it depends on transport parameter values and, possibly, an inversion of direction could be obtained by

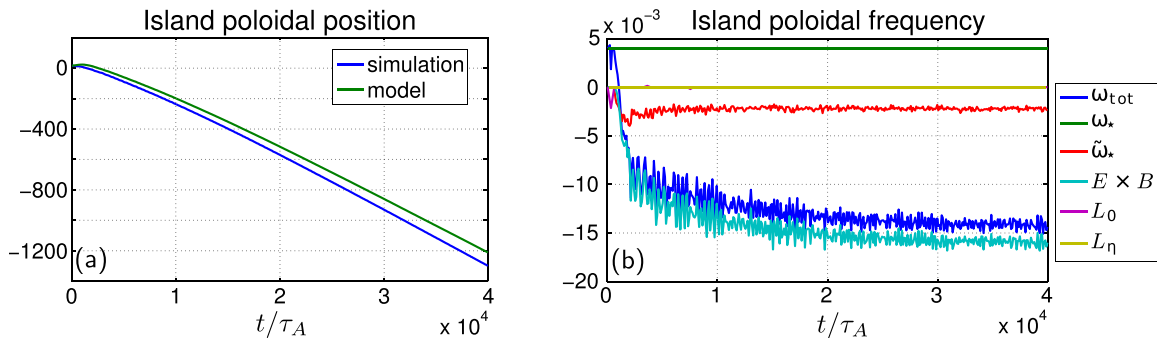


FIG. 10. $\Delta' = -0.45$. (a) Island poloidal position versus time. (b) Island poloidal instantaneous frequency versus time compare with the different contribution of the model Eq. (6).

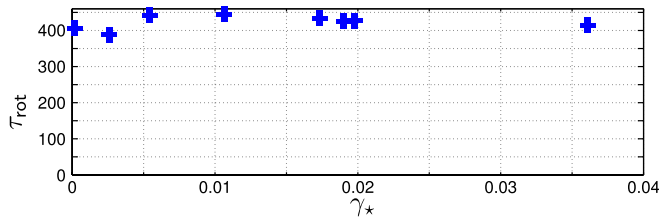


FIG. 11. Period of the island poloidal rotation τ_{rot} versus γ_* .

lowering the viscosity.²⁸ In the present study, we find that for any Δ' value, the island always rotates asymptotically in the ion diamagnetic direction. For lower curvature parameters but identical transport parameters, it was found that it rotates in the electronic diamagnetic direction.²²

More surprisingly, we also observe that the asymptotic island velocity or equivalently the poloidal rotation time $\tau_{rot} = k_1 L_y / \omega_{tot}$ is independent of Δ' and therefore of γ_* (see Fig. 11). Recall that, for large enough Δ' , the tearing is the dominant instability and m_* decreases with Δ' . In other words, the interchange or tearing source levels do not regulate the mean amplitude of the zonal flow. Further analysis shows, however, that the level of fluctuation of the zonal flow is correlated to the interchange source intensity.

VI. PRESSURE PROFILE AND TURBULENCE DRIVEN MAGNETIC ISLANDS

A. Interchange origin of pressure profile flattening

Fig. 10 indicates that the nonlinear diamagnetic velocity does not compensate for the equilibrium one. In other words, the mean pressure profile is not almost flat in the current sheet. In Fig. 12, for the cases $\Delta' = -0.45$ and $\Delta' = +4.02$, the profiles of the pressure are drawn at different times: the end of the QLP or when the nonlinearities become dominant energetically, during the nonlinear phase and in the asymptotic regime where the island velocity becomes roughly constant. In the tearing driven magnetic island case there is a clear flattening of the pressure profile at the resonance while a pressure gradient remains in the turbulence driven magnetic island case. This gradient, denoted by v_*^s , which differs from the imposed equilibrium one, remains constant with time once the nonlinear regime is reached, $v_*^s / v_* \sim 0.4$. Its spatial extension is roughly equal to the island width. The presence of such a gradient is observed in divergence free,

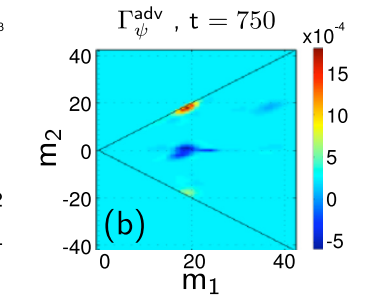
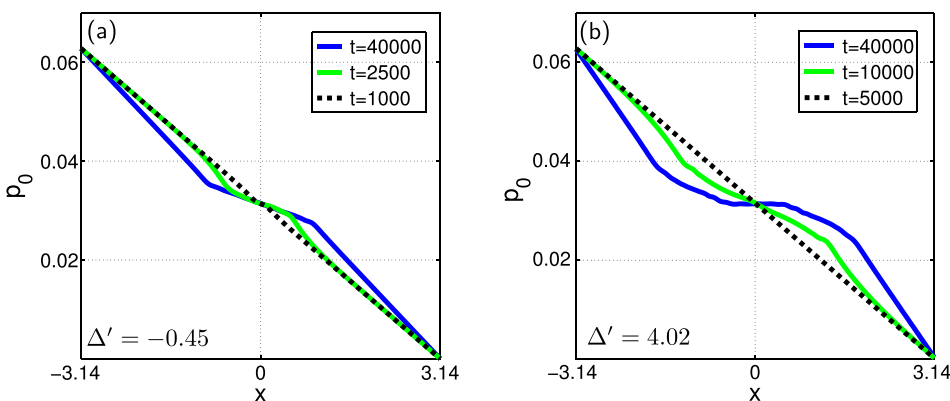


FIG. 13. $\Delta' = -0.45$: Multiscale energy transfers in the pressure equation during the QLP at $t = 750\tau_A$.

non turbulent diffusive heat flow model³¹ when w_s/w_c is below one (w_c being the critical island width above which flattening occurs when explicit parallel conductivity is taken into account). We will verify below that in fact w/w_c is significantly above one even in the QLP. Moreover, Fig. 12 shows that the constant nonlinear pressure gradient inside the island is generated from the QLP.

The constancy of the gradient in the whole island extension is specific to turbulence driven islands. It can be linked to the fact that in the absence of such a pressure gradient the interchange instability would be stabilized inside the island and therefore contradicts the notion of the instability giving rise to the generation of the island. It follows that the gradient should be connected with the level of the small scale turbulence, not the ratio of the diffusivities or equivalently to w_s/w_c .

In fact, during the QLP, the modification of the mean pressure gradient in the vicinity of the resonant surface results from interchange modes coupling, when Δ' is negative. The link with interchange scales can be clearly shown by quantifying the rate of energy transfer between the interchange scales and the largest ones. More globally, in Fig. 13, the energy transfer functions in between all the scales (Refs. 8 and 32) are computed for the pressure equation, namely, $\Gamma_p^{adv}(m_1, m_2, t)$ and $\Gamma_\psi^{adv}(m_1, m_2, t)$. They measure the energy transfer from the modes m_1 and m_2 to the mode $m = m_1 + m_2$ through, respectively, the nonlinearities $[\phi, p]$ and $\hat{\rho}^2[\psi, j]$, *i.e.*, the term of advection of the pressure by the flow and the finite Larmor radius one, in the pressure equation. Let us specify that, by symmetry, the definition of the transfer functions is restricted to the domain $(m_1 \geq 0, |m_2| \leq m_1)$. They satisfy

FIG. 12. Profile of the pressure at different times: (Left) $\Delta' = -0.45$. (Right) $\Delta' = 4.02$.

$$\frac{dE_p}{dt}(m, t) = L_p(m) + \sum_{m=m_1+m_2} (\Gamma_p^{\text{adv}}(m_1, m_2, t) + \Gamma_p^{\hat{\rho}}(m_1, m_2, t)), \tag{7}$$

where $L_p(m)$ is the contribution of the linear terms to the evolution of the energy of the mode m . The impact of $\Gamma_p^{\hat{\rho}}$ is negligible from an energetic point of view compared with Γ_p^{adv} . Fig. 13 shows that interchange scales only contribute to the generation of the large scales ($m \leq 1$) pressure fluctuations and, in particular drive the nonlinear modification of the profile. We also observe that the large scales, interacting with the dominant interchange ones, weaken the growth of the latter. We also show, for completeness, Γ_ψ^{adv} , linked to the bracket $[\phi, \psi]$, which is the dominant transfer function for the magnetic flux evolution equation during the QLP. It allows us to emphasize that magnetic energy transfer occurs from interchange scales to large ones and leads to the growth of a magnetic island.

In the nonlinear phase, this simple picture of multiscale energy transfers disappears and an analysis of that stage is beyond the scope of this paper. However, let us underline, that the bracket $[\phi, p]$ maintains a transfer of energy from the small scales to the large scales, but the small scales are no longer restricted to the dominant unstable interchange ones. Thus, interchange instability directly controls the existence of a constant pressure gradient within the island. From these observations, it follows that a characteristic signature to identify a turbulence driven island could be the presence of a pressure profile with a clear non null constant pressure gradient in the vicinity of the resonance layer along with an island size that is larger than the critical island width w_c .

B. Pressure flattening mechanism in the nonlinear regime

The constancy in time and space of the mean pressure gradient in the nonlinear phase is not intuitive at first glance

because energy transfers do not reduce to a beating of linear modes. However, some heuristic scenario can be proposed. Indeed, the dipole structure of the flow in the nonlinear regime and inside the island redistributes permanently the small scale turbulent structures in the whole island.⁸ Consequently, it tends to spatially homogenize the turbulence inside the island as the rotating island grows and/or saturates. Therefore, the mean pressure gradient which mitigates the turbulence level should be also homogenized.

However interchange instability does not generate a homogeneous small scale turbulence inside the island. This can be clearly observed in Fig. 14 where fluctuations in the island frame of reference $\tilde{\phi}$ and \tilde{p} are shown, the modes $m=0$ and 1 being subtracted to make small scales visible. Interchange scales tend to pile up in the upper part of the island which rotates downward. This poloidal asymmetry indicates that the island rotation influences the distribution of the fluctuations. Simultaneously, fluctuations tend to diffuse along the magnetic field lines at a faster rate: the parallel diffusion time is $\tau_{\parallel} \sim L_y^2 \chi_{\parallel} \sim 7.5$ is much smaller than the time for the island to carry out a poloidal rotation $\tau_{\text{rot}} \sim 400$. The track of the fast parallel diffusion is observed on the \tilde{p} snapshot. Consequently, the energy provided by interchange instability is transferred at large scales preferentially along the magnetic field lines on the edge of the island, in the vicinity of the separatrices. It follows that both, vorticity and current are localized along the separatrices with some important fluctuations close to the X point related to interchange unstable modes (see Fig. 14).

This is consistent with the finding that the mean pressure gradient is constant. Indeed, in the nonlinear regime, the structures of the interchange modes are well localized in the vicinity of the resonance and their amplitudes are weakly fluctuating in time. This is, of course, linked to the characteristic of the mean profiles in the vicinity of the resonance which are invariant since the QL phase. Therefore, it can be postulated that in the nonlinear regime and in the island frame, first, the flux of energy from interchange scales to

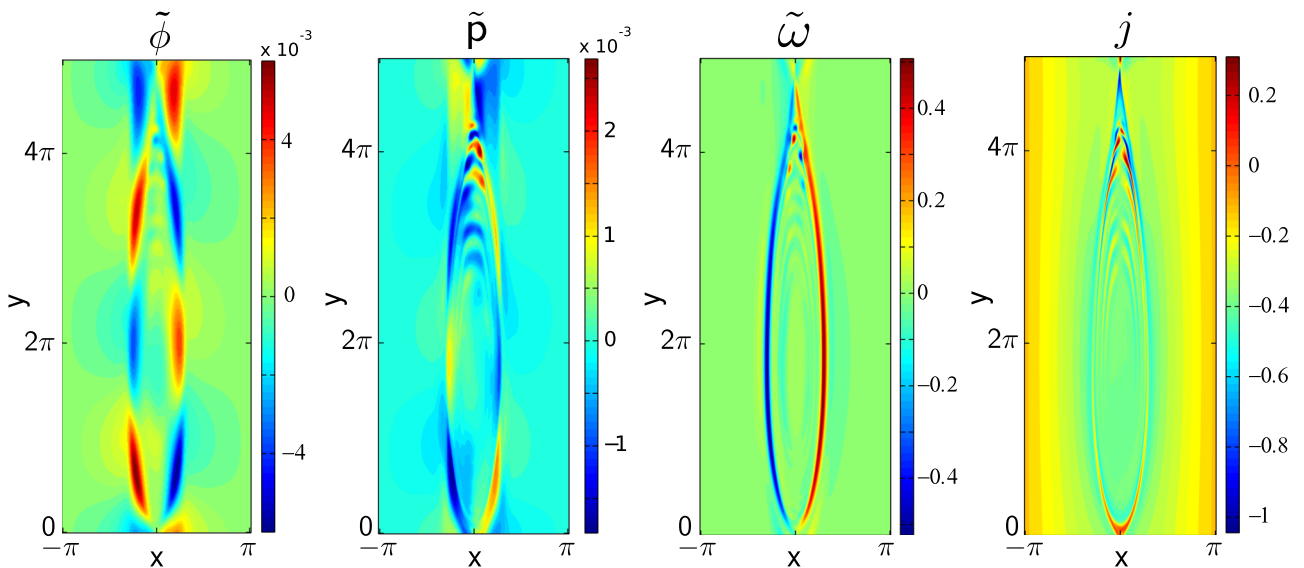


FIG. 14. $\Delta' = -0.45$: Snapshots of fluctuations at $t = 42\ 125\tau_A$. From left to right: $\tilde{\phi}$ and \tilde{p} (removing harmonics $m=0$ and $m=1$), vorticity and current.

island structure is constant in time. Second, the constancy in space relies on a local balance between the level of interchange fluctuations transported along the separatrices and the local mean gradient pressure.

C. A mixing length model

The previous analysis has shown that we can reduce to some extent the dynamics to the interactions of two kinds of structures characterized by their spatial scales, namely the island and the interchange modes. The two scales separation is apparent in Fig. 15 where snapshots of the nonlinear brackets in pressure equation are shown, in the island frame. We clearly observe structures at interchange scales and elongated structures along the field lines. Let us emphasize that in terms of amplitude $\chi_{\parallel} \Delta p \sim \chi_{\parallel} \Delta \phi \gg \hat{\rho}^2[\psi, j]$. In fact χ_{\parallel} contribution tends to compensate partially because the adiabatic response of the electrons is important at small scales, $\phi \sim p$. However, contrary to the non-turbulent case, the remnant non-adiabatic part of the convective term is non-negligible in terms of amplitude compared with $\hat{\rho}^2[\psi, j]$ (see Fig. 15). Finally, it is important to note that in the nonlinear regime, we have a steady state for large scales only in a statistical sense, i.e., by averaging quantities on some island rotation times. Indeed, we expect that for interchange modes $\partial_t \sim \gamma_*^s$.

We can therefore rely on a mixing length theory to obtain some estimates of anomalous transport coefficients at island scales. Let us denote a mean of island scales by an overbar and write $p = \bar{p} + p'$, thus $\bar{p}' = 0$. It follows that $[\phi, p] = [\phi, \bar{p}] + [\phi', p']$. Let us consider dominant fluctuations or cells at interchange scales around the resonance (located in the upper part of graphs in Fig. 14), $\delta p'$ and $\delta \phi'$. As $\tau_{\parallel} \ll \tau_{\text{isl}}$, the stretching of the fluctuations along the separatrices or a field line is fast compared with the island dynamics and we can consider that such fluctuations, on island time scales, are immediately converted into fluctuations at island time scales and denoted by $\delta \bar{p}$ and $\delta \bar{\phi}$. It follows that

$$\begin{aligned} \delta p' l_*^2 &\sim \delta \bar{p} L_y l_*, \\ \delta \phi' l_*^2 &\sim \delta \bar{\phi} L_y l_*, \end{aligned}$$

where $l_* = L_y/m_*$ is an estimate of the extension of interchange cells. The island parallel length is approximately given by L_y . Therefore, noting that $\Delta_{\perp} \sim l_*^{-2}$, $\partial_x \sim l_*^{-1}$ and $\partial_y \sim k_1$, we find

$$\begin{aligned} \overline{[\delta \phi', \delta p']} &\sim k_1 \frac{L_y^2}{l_*^2} [(\delta \bar{\phi})_x \delta \bar{p} - (\delta \bar{p})_x \delta \bar{\phi}] \\ &\sim \chi_1 \Delta_{\perp} \delta \bar{p} - \chi_2 \Delta_{\perp} \delta \bar{\phi}. \end{aligned} \quad (8)$$

The transport coefficients at island scales are $\chi_1 \sim L_y^2 k_1 \delta \bar{\phi} / w_* \sim \delta \phi'$ and $\chi_2 \sim \delta p'$. Noting now that at interchange scales $\gamma_*^s \delta p' \sim [\delta \phi', \delta p'] \sim k_*^2 \delta \phi' \delta p' \sim k_*^2 \delta p'^2$, we obtain $\chi_1 \sim \chi_2 \sim \gamma_*^s / k_*^2$. More generally, anomalous transport coefficient due to nonlinearities are expected to be of the order $\chi_{\perp}^{\text{turb}} = \gamma_*^s / k_*^2 (k_*^s \sim k_*)$.^{6,8}

Consequently, we can conclude that the contribution of interchange source free energy to the diffusion of the pressure at island scales can be taken into account by introducing a large scale anomalous perpendicular diffusivity $\chi_{\perp}^{\text{turb}}$. Let us note that in a recent work, an effective turbulent diffusivity has been computed to account for the drag force acting on the island in the context of ITG turbulence.¹¹ Therefore, one should expect a flattening of the pressure profile when the island size exceeds the critical width $w_c^{\text{turb}} = \sqrt{8} (\chi_{\perp}^{\text{turb}} / \chi_{\parallel})^{1/4} \sqrt{a/k_y} \in [0.26, 0.43]$ for negative Δ' runs. Recall that by using the molecular perpendicular diffusivity, we had obtained a similar range for the set of runs selected in this paper $w_c^{\text{mol}} \in [0.17, 0.34]$. In any case, we always verify $w > w_c = \max(w_c^{\text{mol}}, w_c^{\text{turb}})$ in the present set of simulations, including during the QLP to a large extent and also when Δ' is close to zero, see Fig. 7. A precise study of the threshold above which flattening occurs is out of the scope of this paper. However, the threshold estimate is consistent with the numerical observations.

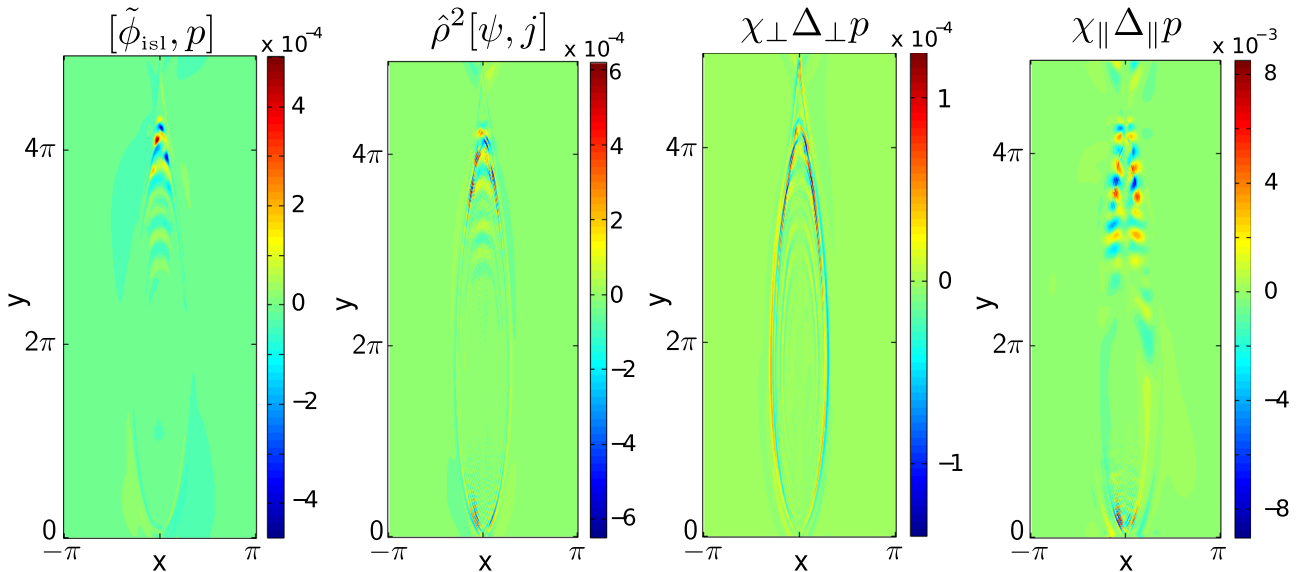


FIG. 15. $\Delta' = -0.45$: Snapshots of dominant contributions in pressure equation at $t = 42 125 \tau_A$ in island rotating frame.

VII. SUMMARY AND DISCUSSION

In this work, we have studied the mechanisms leading to the flattening of the pressure inside magnetic islands, for both, islands that are generated by a tearing instability (including curvature effects), and those generated by small scale interchange turbulence. In the former case, we find that the results agree with earlier theoretical calculations,²⁴ in the limit where, both, island rotation and the induced friction between magnetic and pressure fluctuations at the separatrices are considered. In the case where the islands are generated by turbulence, we also observe a flattening of the pressure inside the magnetic island. An important question is whether or not, we can discriminate such islands from tearing driven ones. This is a necessary step to assess the existence of such islands in the context of tokamak experiments. We find that for turbulence driven islands the mean pressure profile inside them is not completely flat, notably in the resistive layer where the interchange modes grow, and this is a “signature” feature of such islands. This is linked to the fact that a flat profile would kill the interchange instability from which the island itself originates. Another striking fact is that the mean profile gradient inside the island is constant in time and space. This can be interpreted in terms of the setting up of a local equilibrium between the pressure profile gradient and the interchange fluctuation energy levels, the latter being equidistributed in the resistive layer, including the vicinity of separatrices, by advection mechanisms.

We have proposed a mixing length model to account for the small scale interchange turbulence in the theoretical prediction of island flattening. Such kind of models has been extensively used in fluid evolution studies in the context of small scale homogeneous 2D turbulence. This is strictly not applicable in the present context because the turbulence arising from the instability is localized at the resonant surface. However, we have shown that, to some extent, one can introduce an anomalous diffusion coefficient linked to the interchange energy source properties. It gives a prediction of the island size above which flattening of turbulence driven island will occur. In the present study, the simulation results are found to be consistent with the model. Indeed, in all the simulations, the critical island size is exceeded when the system enters in the quasilinear phase. Therefore, a careful numerical investigation of cases where the critical island sizes at saturation do not exceed the predicted critical turbulent island size would be interesting to thoroughly validate the model.

We have also studied the dynamical properties of the magnetic island. In our set of simulations, we have found that the island poloidal rotation velocity is independent of the level of the source which generates the dynamics whether they be the interchange or the tearing instabilities. In the nonlinear asymptotic regime, when $\Delta' < 0$, the interchange growth rate is reduced by a factor independent of the interchange level. Even if the island rotates at the ExB velocity essentially in all the cases, we have shown that there is no ExB flow stabilization of the turbulence. The latter is induced by the nonlinear modification of the mean gradient inside the magnetic island. Finally, by studying the energy transfer between the interchange and island scales, we have

shown that, both, the island and the pressure flattening are directly controlled by interchange instability in the QLP, and no cascade mechanisms are at play. Energy transfers in the fully nonlinear phase are complex and are not presented in this study. In a future work, we will examine the multi-scale energy transfers, including cascade mechanisms in the nonlinear regime, which modify the turbulence characteristics^{8,10} and possibly the transport properties.

ACKNOWLEDGMENTS

This work was supported by the European Communities under the contract of Association between EURATOM and CEA. The views and opinions expressed herein do not necessarily reflect those of the European Commission.

- ¹X. Garbet, P. Mantica, C. Angioni, E. Asp, Y. Baranov, C. Bourdelle, R. Budny, F. Crisanti, G. Cordey, L. Garzotti *et al.*, *Plasma Phys. Controlled Fusion* **46**, B557 (2004).
- ²A. K. Sundaram and A. Sen, *Phys. Rev. Lett.* **44**, 322 (1980).
- ³A. Sen and A. K. Sundaram, *Phys. Fluids* **24**, 1303 (1981).
- ⁴S.-I. Itoh, K. Itoh, and M. Yagi, *Phys. Rev. Lett.* **91**, 045003 (2003).
- ⁵A. Furuya, S.-I. Itoh, and M. Yagi, *Contrib. Plasma Phys.* **40**, 375 (2000).
- ⁶A. Furuya, S.-I. Itoh, and M. Yagi, *J. Phys. Soc. Jpn.* **70**, 407 (2001).
- ⁷M. Muraglia, O. Agullo, S. Benkadda, X. Garbet, P. Beyer, and A. Sen, *Phys. Rev. Lett.* **103**, 145001 (2009).
- ⁸M. Muraglia, O. Agullo, S. Benkadda, M. Yagi, X. Garbet, and A. Sen, *Phys. Rev. Lett.* **107**, 095003 (2011).
- ⁹W. A. Hornsby, M. Siccino, A. G. Peeters, E. Poli, A. P. Snodin, F. J. Casson, Y. Camenen, and G. Szepesi, *Plasma Phys. Controlled Fusion* **53**, 054008 (2011).
- ¹⁰J. Li, Y. Kishimoto, and Z. X. Wang, *Phys. Plasmas* **21**, 020703 (2014).
- ¹¹A. Ishizawa and F. L. Waelbroeck, *Phys. Plasmas* **20**, 122301 (2013).
- ¹²M. Yagi, S.-I. Itoh, K. Itoh, M. Azumi, P. H. Diamond, A. Fukuyama, and T. Hayashi, *J. Plasma Fusion Res.* **2**, 025 (2007).
- ¹³F. Waelbroeck, F. Militello, R. Fitzpatrick, and W. Horton, *Plasma Phys. Controlled Fusion* **51**, 015015 (2009).
- ¹⁴A. Ishizawa and N. Nakajima, *Nucl. Fusion* **47**, 1540 (2007).
- ¹⁵A. Ishizawa and N. Nakajima, *Phys. Plasmas* **17**, 072308 (2010).
- ¹⁶R. J. La Haye and O. Sauter, *Nucl. Fusion* **38**, 987 (1998).
- ¹⁷A. Isayama, G. Matsunaga, Y. Hirano, and the JT-60 Team, *J. Plasma Fusion Res.* **8**, 1402013 (2013).
- ¹⁸B. D. Scott, A. B. Hassam, and J. F. Drake, *Phys. Fluids* **28**, 275 (1985).
- ¹⁹M. Ottaviani, F. Porcelli, and D. Grasso, *Phys. Rev. Lett.* **93**, 075001 (2004).
- ²⁰D. Biskamp, *Magnetic Reconnection in Plasmas* (Cambridge University Press, 2000).
- ²¹E. G. Harris, *Nuovo Cim.* **23**, 115 (1962).
- ²²M. Muraglia, O. Agullo, M. Yagi, S. Benkadda, P. Beyer, X. Garbet, S.-I. Itoh, K. Itoh, and A. Sen, *Nucl. Fusion* **49**, 055016 (2009).
- ²³K. Takeda, O. Agullo, S. Benkadda, A. Sen, N. Bian, and X. Garbet, *Phys. Plasmas* **15**, 022502 (2008).
- ²⁴R. Fitzpatrick, *Phys. Plasmas* **2**, 825 (1995).
- ²⁵T. Vosliou, O. Agullo, P. Beyer, M. Yagi, S. Benkadda, X. Garbet, K. Itoh, and S.-I. Itoh, *Phys. Plasmas* **18**, 062302 (2011).
- ²⁶K. J. Gibson, N. Barratt, I. Chapman, N. Conway, M. R. Dunstan, A. R. Field, L. Garzotti, A. Kirk, B. Lloyd, H. Meyer *et al.*, *Plasmas Phys. Controlled Fusion* **52**, 124041 (2010).
- ²⁷S. Gunter, S. Schade, M. Maraschek, S. D. Pinches, E. Strumberger, R. Wolf, Q. Yu, and ASDEX Upgrade Team, *Nucl. Fusion* **40**, 1541 (2000).
- ²⁸S. Nishimura, S. Benkadda, M. Yagi, S.-I. Itoh, and K. Itoh, *Phys. Plasmas* **15**, 092506 (2008).
- ²⁹K. Itoh, S.-I. Itoh, P. H. Diamond, T. S. Hahm, A. Fujisawa, G. R. Tynan, M. Yagi, and Y. Nagashima, *Phys. Plasmas* **13**, 055502 (2006).
- ³⁰R. E. Waltz, G. D. Kerbel, and J. Milovich, *Phys. Plasmas* **1**, 2229 (1994).
- ³¹J. A. Snape, K. J. Gibson, T. O’Gorman, N. C. Barratt, K. Imada, H. R. Wilson, G. J. Tallents, I. T. Chapman, and the MAST team, *Plasmas Phys. Controlled Fusion* **54**, 085001 (2012).
- ³²A. Alexakis, P. D. Mininni, and A. Pouquet, *Phys. Rev. E* **72**, 046301 (2005).